Magnetic Live Surface Layers in Fe/Cu(100)

J. Thomassen, F. May, B. Feldmann, M. Wuttig,[a] and H. Ibach
Institut für Grenzflächenforschung und Vakuumphysik, Forschungszentrum Jülich, Postfach 1913, D-5170 Jülich, Federal Republic of Germany
(Received 8 October 1992)

The magnetic properties of Fe films epitaxially grown on Cu(100) have been correlated to their structure and morphology. Strained fcc iron films with thicknesses between 5 and 11 monolayers (ML) are ferromagnetically ordered at the surface with a perpendicular orientation of the magnetic moment, whereas the bulk of the films remains paramagnetic. The surface magnetism is related to an expanded interlayer distance at the surface. With the onset of dislocation formation at about 11 ML, the films become magnetic in the bulk and the magnetization switches to in-plane orientation.

PACS numbers: 75.70.Ak, 68.55.Jk, 75.30.Gw, 75.30.Pd

Magnetic exchange coupling depends strongly on interatomic distances. For example, for fcc iron, a nonmagnetic phase, a high-spin or a low-spin phase, or an antiferromagnetic phase is predicted to be stable depending on the lattice parameter [1–3]. However, experimental tests of such predictions are difficult, if not impossible with bulk material, in particular when the interest is in phases which are unstable at room temperature. Epitaxial growth of thin films offers the unique opportunity to force the system into metastable, yet ordered states of matter, controlled by the choice of the substrate, the growth conditions, and the film thickness. In that regard the epitaxially grown Fe films on Cu(100) have attracted considerable interest because of both their structural richness [4–7] and their unusual magnetic properties [8–11]. The latter encompass a strong magnetic anisotropy which orients the magnetic moment perpendicularly to the film [12,13]. Several authors have reported on correlations between the morphology of Fe films and their magnetic properties [14,15], albeit in qualitative terms so far. Here we report on an attempt for a complete and quantitative investigation of the growth mode, the crystallographic structure and the magnetic properties as a function of film thickness, with experimental techniques applied *in situ* to the same epitaxial system. This study shows that the reorientation of the magnetic anisotropy from perpendicular to in plane is directly related to a structural transition of the iron films. We demonstrate also that the magnetism of pseudo fcc-type Fe films grown in the layer-by-layer growth mode is not a property of the bulk of the film but is rather confined to the surface layer. The ferromagnetism of the surface layer is apparently correlated with the expanded interatomic distance of the iron atoms near the surface.

The iron films were grown at room temperature with typical evaporation rates of 1–2 ML/min (ML denotes monolayer). The pressure during evaporation was always below 2×10^{-8} Pa. The film growth was monitored by measuring the medium energy electron diffraction (MEED) intensities of several diffracted beams during Fe deposition. These measurements and an additional calibration of the evaporation rate by a quartz-crystal microbalance allow a thickness determination with an accuracy of 0.3 ML. The structure of the iron films was determined by a quantitative low energy electron diffraction (LEED) analysis of the measured intensity versus energy curves [16]. The magnetic properties were investigated using the surface magneto-optic Kerr effect (SMOKE) for recording hysteresis loops in longitudinal and polar geometry employing a polarization modulation technique [17,18]. The light source was a He-Ne laser with a wavelength of 632.8 nm.

In Fig. 1, polar and longitudinal Kerr ellipticity curves for a 10-ML-thick film at $T=170$ K are shown. In the longitudinal geometry no hysteresis is observed within the experimental accuracy, whereas the polar measurement

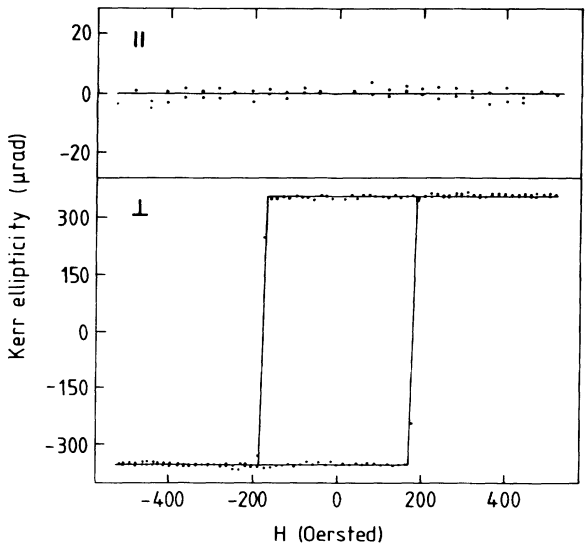

FIG. 1. Kerr ellipticity curves for a 10-ML-thick film at $T=170$ K recorded in longitudinal (upper curve) and polar geometry (lower curve). The angle of incidence for the longitudinal and polar measurements was 65° and 25° against the surface normal, respectively. The azimuthal direction of incidence was chosen along the [110] direction.

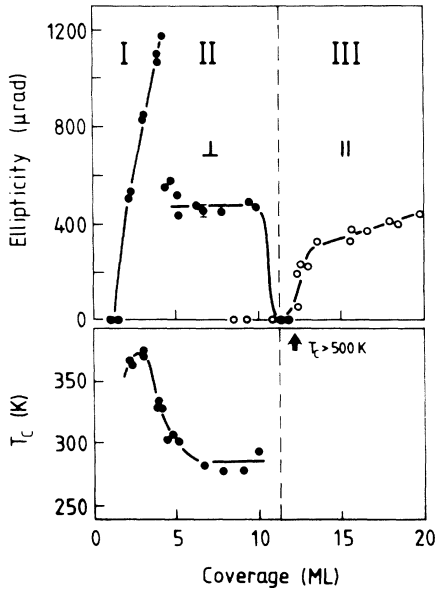

FIG. 2. Upper curve: Thickness dependence of the Kerr ellipticities at saturation extrapolated to $T=0$ K. The solid and open circles denote the ellipticities obtained from hysteresis loops recorded in polar and longitudinal geometry, respectively. The error bar is indicated in the figure. The longitudinal ellipticities are smaller than the polar ellipticities due to the reduced sensitivity of the longitudinal Kerr effect [30]. For the chosen angles of incidence, a value of approximately 8 is calculated for the ratio between the magnitudes of the ellipticities. Three regions with different magnetic properties and different orientation of the magnetic anisotropy can be distinguished. Lower curve: Thickness dependence of the Curie temperature T_C. Around 11 ML the Curie temperatures jump to values above 500 K. The experimental error lies within the size of the dots.

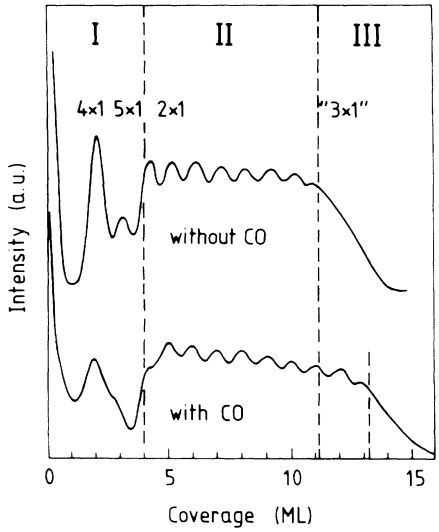

FIG. 3. MEED curves of the specular beam for growth under clean ultrahigh vacuum conditions ($p_{tot}=1\times10^{-8}$ Pa, upper curve) and for a CO partial pressure of 7×10^{-8} Pa (lower curve). The curves were recorded with an electron energy of 3 keV and at an angle of incidence of 8.9° with the sample surface. Three regions of different growth behavior can be distinguished. With increasing film thickness four different superstructures evolve.

gives a perfectly square loop indicating a perpendicular magnetic anisotropy. A series of SMOKE experiments was performed for a large number of films with different thicknesses. For each thickness, a sequence of polar or longitudinal Kerr rotation (θ_K) and ellipticity (ε_K) hysteresis loops was recorded for temperatures between 110 K and the Curie temperature T_C of the film. Figure 2 summarizes the results of these experiments. The ellipticities plotted in the upper part of Fig. 2 were obtained by extrapolating the saturation values ε_K^s of the Kerr ellipticities to $T=0$ K using the known $T^{3/2}$ dependence at low temperature. The Curie temperatures shown in the lower part of Fig. 2 were determined by extrapolating the ellipticities at saturation to $\varepsilon_K^s=0$ [19].

From the thickness dependence of the Curie temperatures and the Kerr ellipticities, three regions with different magnetic properties can be distinguished. Up to about 4 ML, a perpendicular anisotropy with Kerr ellipticities increasing linearly with film thickness is found. The Curie temperatures in this region show a maximum around 3 ML in agreement with measurements by Stampanoni [20]. Around 4 ML, the Kerr signal decreases sharply indicating a change in the magnetic properties at this thickness. At about 11 ML the magnetization switches from perpendicular to in-plane orientation. In addition the Curie temperature rises to above 500 K. The Kerr ellipticities in this region again increase linearly with coverage. A linear increase as observed in regions I and III is expected for a homogeneously magnetized film whereas between 5 and 11 ML the Kerr ellipticity remains practically constant.

The three different regimes of magnetic behavior are correlated with different regimes of growth (Fig. 3). Layer-by-layer growth characterized by regular intensity oscillations of the diffracted intensity is found between 5 and 11 ML (region II). Above this thickness the formation of misfit dislocations leads to 3D island growth connected with a drastic decrease in the MEED intensity [21]. The 3D islands grow with bcc structure in the [110] orientation [22]. The first region up to about 5 ML is characterized by a deep intensity minimum at 1 ML. This behavior in the initial stage of growth is indicative of iron agglomeration. This agglomeration has already been found by x-ray photoemission spectroscopy forward scattering [23,24] and was confirmed by diffusion experiments [21] and a scanning tunneling microscopy study [25]. In agreement with earlier work [4,5] we also find two different superstructures, namely, a 4×1 structure around 2 ML and a 5×1 structure around 4 ML. Connected with the coalescence of iron islands around 5 ML, a change in structure is found which leads to the appear-

ance of a 2×1 superstructure between 5 and 8 ML. Above 12 ML, the formation of the bcc (110) islands leads to the appearance of additional spots in the LEED pattern close to the positions expected for a 3×1 structure. All superstructures are intrinsic properties of the clean iron films. Contamination-induced superstructures are only observed for considerably higher concentrations of contaminants.

The data imply a close correlation between film morphology and the magnetic properties. In order to prove that the correlation is not incidental we have extended the regime of layer-by-layer growth using CO as a surfactant. A CO background pressure of 7×10^{-8} Pa was maintained during Fe deposition. This shifts the onset of dislocation formation from 11 to above 13 ML (see lower portion of Fig. 3). Concomitant with the shift in the structural transition is the shift in the reorientation of the magnetic polarization from perpendicular to parallel as shown in Fig. 4. For 12.5 ML a hysteresis in the longitudinal Kerr signal is present only for the films grown without CO. On the other hand, for 11.5 ML the polar Kerr signal is indicative of a perpendicular magnetic anisotropy in the case of extended layer-by-layer growth. We have checked that the differences regarding the orientation of the magnetic anisotropy are not induced by CO adsorption after the deposition of the Fe films. Therefore we can conclude that the change of the magnetic properties is directly linked to the structural rearrangement which accompanies the breakdown of layer-by-layer growth.

The relatively small and constant Kerr ellipticity between 5 and 11 ML indicates that the bulk of the film does not contribute to the observed Kerr signal. Hence

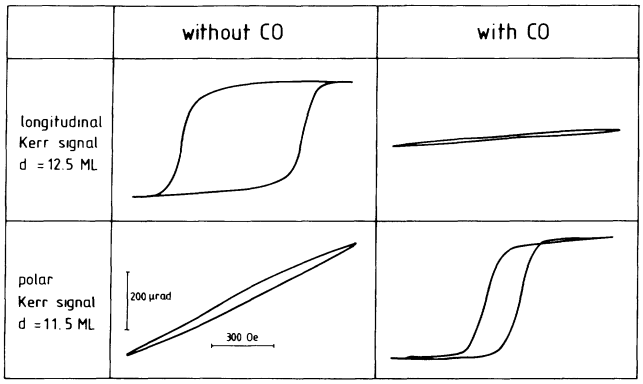

FIG. 4. Kerr ellipticity loops recorded at 170 K in polar and longitudinal geometry for different iron films grown under clean ultrahigh vacuum conditions and for a CO partial pressure of 7×10^{-8} Pa. The films deposited with simultaneous CO exposure maintain layer-by-layer growth up to 13 ML, whereas the critical thickness for dislocation formation is 11 ML without CO (Fig. 3). The scaling of the horizontal and vertical axes is indicated in the lower right panel. The x axis in the lower right panel is expanded by a factor of 5.

the magnetism must be localized either at the Fe-Cu interface or at the surface. We found that CO exposure of 0.5 L (langmuir, 1 L$=10^{-6}$ Torrs) lowers the Curie temperature by 40 K. This is evidence that the magnetism is essentially localized at or near the surface of the films. Furthermore, we can exclude an antiferromagnetic coupling between successive iron layers for the temperature range investigated ($T > 110$ K). In this case, an oscillation of the Kerr ellipticity with film thickness should be observed as the net magnetic moment of films with even and odd numbers of layers would be different. Thus the bulk of the films is either paramagnetic or antiferromagnetic, but with a Néel temperature below 110 K.

The formation of a ferromagnetically ordered ("live") surface layer is directly correlated to the film structure. This can be inferred from the results of a quantitative structure determination by LEED intensity analysis, which we have performed for films with thicknesses of 8, 11, and 15 ML. The analysis shows that for the 8- and 11-ML films the distance between the surface and the subsurface layer is significantly expanded by about 0.1 $\pm$0.02 Å. While the second interlayer distance is still slightly expanded to 1.80 Å, the deeper interlayer distances are close to the value of 1.77 Å expected for a tetragonal phase obtained from a laterally compressed fcc lattice [16]. These numbers are in qualitative agreement with results obtained in earlier work for film thicknesses of 6, 10, and 12 ML, respectively [6,14,26]. We note that an expansion of the interlayer distance at the surface is rather unusual, since (100) surfaces of fcc transition metals typically display a small contraction. The ferromagnetic behavior of the expanded surface layers with an expanded interatomic distance is consistent with the results of theoretical studies on bulk fcc iron [1–3]. From our CO codeposition experiments we can further conclude that the range of thicknesses, where the strained fcc structure exists, is influenced by small amounts of surface contamination. In addition, the structure of the films is dependent on the substrate temperature during growth and on the sample preparation [15,24]. This might explain the differences between the critical thicknesses obtained by various groups [10,12]. Under the growth conditions chosen, the interdiffusion between Fe and Cu is marginal [21,24]. Our results therefore describe the intrinsic properties of strained fcc iron on Cu(100). This is in contrast to results reported earlier where a correlation between structure and magnetism was claimed for films grown at elevated temperatures (420–460 K) [27,28]. At these temperatures, significant interdiffusion has been found [24]. This explains why an irreversible change of the magnetic properties after 1 h in ultrahigh vacuum was observed in this study. Our results are not at variance with experiments by Stampanoni [20], where a constant spin polarization of photoemitted electrons for film thicknesses between 5 and about 14 ML was found.

Several other observations are explained by magnetic

live surface layers on top of a nonmagnetic iron film. The relatively low Kerr ellipticity, for example, is consistent with a very thin magnetically active layer. We have determined the critical exponent β for the surface magnetization to be approximately 0.17 ± 0.03 using a temperature range between $0.9T_C$ and $0.99T_C$. This value is much closer to the value found for two-dimensional magnetic films than for bulklike films where values around $\frac{1}{3}$ are reported [29]. Magnetic live surface layers can also account for the observed absence "of ferromagnetism in the usual sense" in other work [15]. Most importantly, our model explains why the critical thickness is so large. Since the magnetization is confined to the surface, the demagnetization energy does not increase with the film thickness. The magnetization switches to in-plane orientation after the substrate-induced strain is relieved by the formation of dislocations and the film structure is changed to bcc beyond deposition of 11 ML.

In conclusion, we have shown that the specific structures forced upon the iron films by epitaxy and the magnetic properties of these films are intimately related. Most importantly, a new, structurally well characterized phase of iron with a paramagnetic bulk and a ferromagnetically ordered surface layer is identified. Further theoretical investigations ellucidating quantitative details and the range of epitaxial forces under which the new magnetic phase can exist should be highly rewarding.

[a]Author to whom correspondence should be addressed.

[1] C. S. Wang, B. M. Klein, and H. Krakauer, Phys. Rev. Lett. **54**, 1852 (1985).
[2] F. J. Pinski, J. Staunton, B. L. Gyorffy, D. D. Johnson, and G. M. Stocks, Phys. Rev. Lett. **56**, 2096 (1986).
[3] V. L. Moruzzi, P. M. Marcus, K. Schwarz, and P. Mohn, Phys. Rev. B **34**, 1784 (1986).
[4] W. Daum, C. Stuhlmann, and H. Ibach, Phys. Rev. Lett. **60**, 2741 (1988).
[5] C. Egawa, E. M. McCash, and R. F. Willis, Surf. Sci. **215**, L271 (1989).
[6] H. Landskron, G. Schmidt, K. Heinz, K. Müller, C. Stuhlmann, U. Beckers, M. Wuttig, and H. Ibach, Surf. Sci. **256**, 115 (1991).
[7] H. Magnan, D. Chandesris, B. Villette, O. Heckmann, and J. Lecante, Phys. Rev. Lett. **67**, 859 (1991).
[8] D. Pescia, M. Stampanoni, G. L. Bona, A. Vaterlaus, R. F. Willis, and F. Meier, Phys. Rev. Lett. **58**, 2126 (1987).
[9] W. A. A. Macedo and W. Keune, Phys. Rev. Lett. **61**, 475 (1988).
[10] D. P. Pappas, K. P. Kämper, and H. Hopster, Phys. Rev. Lett. **64**, 3179 (1990).
[11] F. J. Himpsel, Phys. Rev. Lett. **67**, 2363 (1991).
[12] C. Liu, E. R. Moog, and S. D. Bader, Phys. Rev. Lett. **60**, 2442 (1988).
[13] M. Stampanoni and R. Allenspach, J. Magn. Magn. Mater. **104-107**, 1805 (1992).
[14] S. H. Lu, J. Quinn, D. Tian, F. Jona, and P. M. Marcus, Surf. Sci. **209**, 364 (1989).
[15] P. Xhonneux and E. Courtens, Phys. Rev. B **46**, 556 (1992).
[16] M. Wuttig and J. Thomassen, Surf. Sci. (to be published).
[17] J. Badoz, M. Billardon, J. C. Canit, and M. F. Russell, J. Opt. **8**, 373 (1977).
[18] S. H. Jasperson and S. E. Schnatterly, Rev. Sci. Instrum. **40**, 761 (1969).
[19] J. Kohlhepp, H. J. Elmers, S. Cordes, and U. Gradmann, Phys. Rev. B **45**, 12287 (1992).
[20] M. Stampanoni, Appl. Phys. A **49**, 449 (1989).
[21] J. Thomassen, B. Feldmann, and M. Wuttig, Surf. Sci. **264**, 406 (1992).
[22] M. Wuttig, F. May, J. Thomassen, B. Feldmann, H. Zillgen, A. Brodde, H. Hannemann, and H. Neddermeyer (to be published).
[23] S. A. Chambers, T. J. Wagener, and J. H. Weaver, Phys. Rev. B **36**, 8992 (1987).
[24] D. A. Steigerwald, I. Jacob, and W. F. Egelhoff, Jr., Surf. Sci. **202**, 472 (1988).
[25] M. Brodde and H. Neddermayer (to be published).
[26] Y. Darici, J. Marcano, H. Min, and P. A. Montano, Surf. Sci. **182**, 477 (1987).
[27] S. D. Bader and E. R. Moog, J. Appl. Phys. **61**, 3729 (1987).
[28] P. A. Montano, G. W. Fernando, B. R. Cooper, E. R. Moog, H. M. Naik, S. D. Bader, Y. C. Lee, Y. N. Darici, H. Min, and J. Marcano, Phys. Rev. Lett. **59**, 1041 (1987).
[29] U. Gradmann, J. Magn. Magn. Mater. **100**, 481 (1991).
[30] J. Zak, E. R. Moog, C. Liu, and S. D. Bader, J. Magn. Magn. Mater. **89**, 107 (1990).